

文章编号: 1001-4888(2024)03-0287-08

Mbone 仿真骨压缩及扭转生物力学等效性研究*

李钰^{1,2}, 辛鹏³, 刘谟语^{2,4}, 汪芷萱², 王君^{2,4,5}, 郇勇^{2,4}

(1. 中国农业大学 工学院, 北京 100083; 2. 中国科学院力学研究所 非线性力学国家重点实验室, 北京 100190;

3. 中国人民解放军南部战区总医院 骨科, 广东广州 510010; 4. 中国科学院大学 工程科学学院, 北京 100049;

5. 之江实验室 前沿基础研究中心, 浙江杭州 311121)

摘要: 在临床应用及骨力学研究中, 尸体骨样品稀缺且一致性较差, 因此力学等效仿真骨不可或缺。美国 Sawbones 合成骨是目前世界上最具认可度的力学等效仿真骨, 但其模型基于西方人开发, 与中国人骨型有差异, 尤其是股骨前弓角和前倾角与中国人有较大不同。本文旨在通过生物力学实验, 研究基于中国人骨特点自研的新型力学等效仿真骨 Mbone 股骨的压缩及扭转力学性能, 验证其力学等效性。本文测试并对比了新型自研力学等效仿真骨 Mbone 股骨和 Sawbones 股骨的压缩及扭转力学性能, 结果显示: 受压时, Mbone 股骨压缩刚度比 Sawbones 略高 7.2%, 且其压缩破坏载荷在尸体骨范围内, 破坏后呈现出与临床相符的股骨颈骨折; Mbone 股骨内侧中段偏后方的压应变明显高于 Sawbones, 其他 15 个区域压应变与 Sawbones 高度一致。受扭时, Mbone 股骨内旋扭转刚度比 Sawbones 略低 6.7%, 外旋扭转刚度比 Sawbones 低 18.3%。Mbone 力学等效仿真股骨在压缩及扭转力学性能上均表现出良好的力学等效性, 且更贴合中国人骨型, 因此认为其可以替代进口产品作为尸体骨的力学等效模型。

关键词: 力学等效; 压缩; 扭转; Mbone; Sawbones; 股骨

中图分类号: O348

文献标识码: A

DOI: 10.7520/1001-4888-23-170

0 引言

在骨力学实验研究中, 尸体骨样品不易获取, 且难以保持样品一致性^[1]。因此, 与尸体骨力学性能相仿的力学等效仿真骨不可或缺。力学等效仿真骨不仅需要还原骨的外形特点, 还要模拟骨的力学特性, 如骨的压缩刚度、扭转刚度、弯曲刚度、远近端应力分布规律、局部植入物与骨间的载荷传递、螺钉旋入扭矩等^[2]。在骨科临床及骨力学研究中, 力学等效仿真骨可以用于术前模拟、操作培训以及骨-植入物力学性能测试等。

目前市面上认可度最高、应用最广泛的力学等效仿真骨是 Sawbones 第四代合成骨, 其皮质骨材料为环氧树脂和短玻璃纤维的复合材料, 松质骨材料为聚氨酯泡沫。ZDERO 等^[3]回顾了验证 Sawbones 力学等效的相关研究, 从材料性能、整骨性能、骨科应用性能等方面讨论了其力学性能。第四代 Sawbones 皮质骨材料的纵向压缩弹性模量约为 15.8 GPa, 强度可达到 107 MPa, 这与人体皮质骨的力学性能相当^[4]。有研究测试了 Sawbones 股骨整骨在压缩、扭转工况下的刚度、强度和应变分布, 验证了其整骨力学性能的等效性^[5]。CHONG 等^[6]验证了 Sawbones 股骨在髋关节置换术后疲劳性能测试中的有效价值。LAMB 等^[7]研究发现 Sawbones 合成股骨和尸体股骨植入假体后的扭转刚度、骨折扭矩及

* 收稿日期: 2023-08-12; 修回日期: 2023-10-07

通信作者: 郇勇(1975-), 男, 博士, 正高级工程师。主要从事实验力学研究。Email: huany@lnm.imech.ac.cn

王君(1995-), 女, 博士, 助理研究员。主要从事生物力学研究。Email: wangjun1995@zhejianglab.com

骨折模式相似,证实了 Sawbones 股骨模型可以在一定条件下作为假体周围骨折研究的合理选择。目前 Sawbones 合成骨广泛应用于创伤骨科、脊柱外科、关节外科及运动医学等领域,代替尸体骨用于各种钢板、内固定材料的力学测试^[8-13]。但 Sawbones 合成骨内部聚氨酯泡沫密度均匀,而真实松质骨是具有梯度变化的^[14-16]。此外,该合成骨以欧美人为模板进行制作,虽然区分不同大小型号,但其骨骼形态参数与中国人骨骼的差距较大,尤其是作为人体下肢重要承载部位的股骨。中国人与西方人在股骨形态上的差异主要有 2 点:一是中国人股骨颈前倾角较大,二是中国人有明显的股骨前弓角。股骨颈前倾角指的是股骨颈轴线与人体冠状面的夹角,前弓角则是指股骨上段向前弯曲的角度,两者测量方法如图 1 所示。中国人股骨颈前倾角约为 14.3° ,前弓角约为 10.6° ^[17-18];而西方人的股骨颈前倾角平均为 11.4° ,前弓角仅为 5.8° ^[19],因此,研制基于中国人骨型的力学等效仿真股骨十分必要。

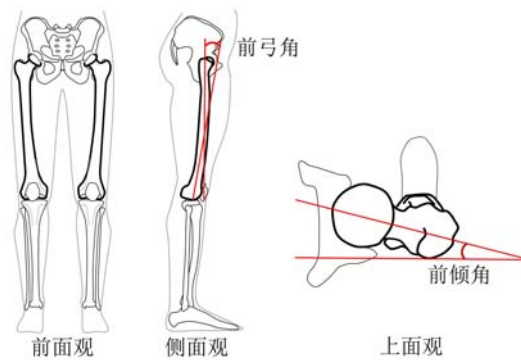


图 1 股骨形态参数:前弓角及前倾角

Fig. 1 Femoral morphological parameters: anterior arch angle and anteversion angle

中国科学院力学研究所自主研发了一种基于中国人骨的新型力学等效仿真骨 Mbone,其松质骨为等效梯度微结构,皮质骨为自行研制的复合材料,制作方式如图 2 所示。仿真骨的力学等效性需要多角度、全方位验证,而在骨科植入物研发中,股骨压缩及扭转性能备受关注。因此,本文主要通过生物力学实验方法研究新型力学等效仿真骨 Mbone 股骨的压缩及扭转力学性能等效性。

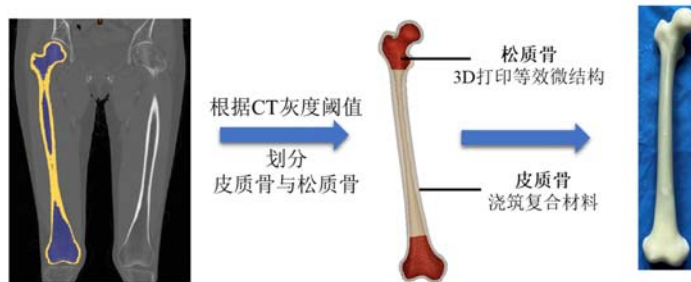


图 2 Mbone 仿真股骨制作流程

Fig. 2 Production process of Mbone femur

1 研究方法

由于尸体骨样品稀缺不易获取,本文以目前力学等效认可度最高的 Sawbones 仿真股骨作为参考,间接验证 Mbone 股骨的压缩及扭转力学等效性,并调研了以往文献中尸体股骨力学测试数据加以佐证。使用 Instron E10000 材料试验机对 Mbone 力学等效仿真股骨及 Sawbones 第四代合成股骨进行压缩及扭转力学性能测试,对比并分析两者异同。

Mbone 和 Sawbones 力学等效仿真股骨实验样品及尺寸如图 3 所示,其中 Mbone 为右侧股骨, Sawbones 为左侧股骨,两者结构为镜像关系。经测量, Mbone 股骨的前弓角(11°)及前倾角(15°)明显大于 Sawbones 股骨(前弓角 5° 、前倾角 10°),且 Sawbones 的股骨总长及股骨颈长度大于 Mbone。

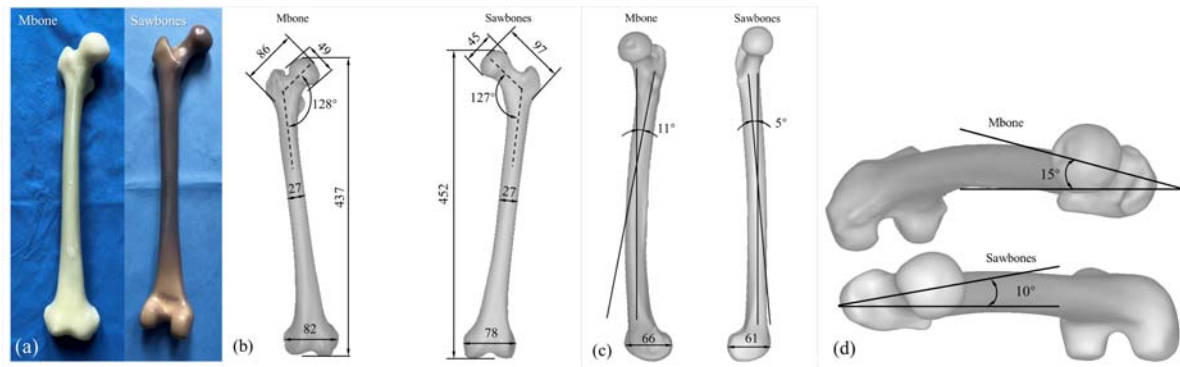


图 3 Mbone 股骨与 Sawbones 股骨样品(单位: mm):(a)实验样品;(b)前面观;(c)前弓角;(d)前倾角

Fig. 3 Mbone femur and Sawbones femur(unit: mm):(a) experimental samples;

(b) front view;(c) anterior arch angle;(d) anteversion angle

1.1 仿真股骨整骨压缩力学实验

将股骨髁锯除后把股骨远端包埋在牙托粉中固化成圆柱体,使用螺钉将股骨远端圆柱体固定在筒状夹具中,通过法兰盘与试验机相连,远端固定,近端加载。装夹角度参考站立时的股骨力线,保证股骨头中心与股骨远端中心的连线在加载轴线上,模型固定方式如图 4 所示。

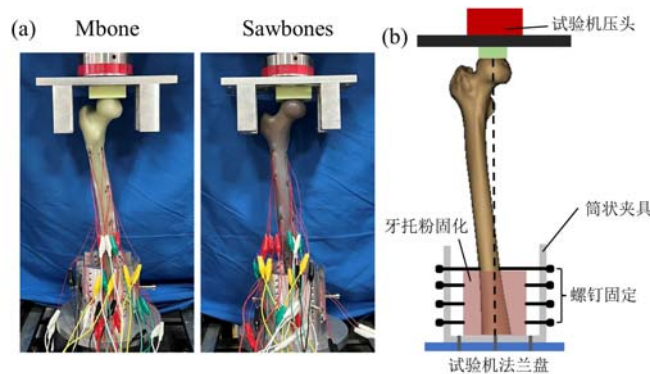


图 4 (a) Mbone 股骨与 Sawbones 股骨压缩实验;(b)压缩固定示意图

Fig. 4 (a) compression test of Mbone femur and Sawbones femur;(b) compressed fixed diagram

另外,参照 Gruen 分区在股骨表面 16 个点位上沿股骨干轴线方向粘贴电阻应变片,并通过导线连接至应变采集系统,分区如图 5 所示。

实验前以 150N 的垂直载荷进行 3 次重复预加载,消除装夹初始不稳的现象。实验第一阶段压缩至约 2000N,模拟人体行走状态下承受 3 倍体重时的压缩负载^[20],同步触发材料试验机和应变采集系统并采集时间、载荷、应变信息;第二阶段压缩至 Mbone 股骨破坏,模拟股骨压缩骨折情况,采集载荷及位移信息。

1.2 仿真股骨整骨扭转力学实验

用扭转专用夹具将股骨模型固定在试验机上,通过调整夹具位置使股骨头中心与股骨远端连线在试验机轴线上,扭转时保证股骨旋转中心在股骨头中心,模型固定方式如图 6 所示。分别以 1N·m 逆时针扭矩及顺时针扭矩进行 3 次重复预加载,然后施加压缩载荷 600N,保持压缩载荷恒定,继续逆时针或顺时针加载至 15N·m,模拟人体下肢内旋及外旋状态^[5, 21]。

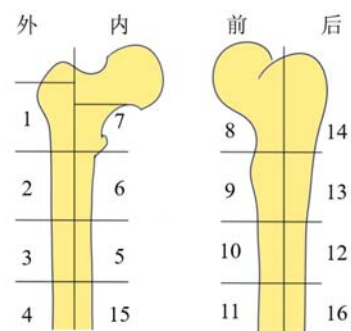


图 5 基于 Gruen 分区的 16 个应变测量点位

Fig. 5 16 strain measurement points based on Gruen partition

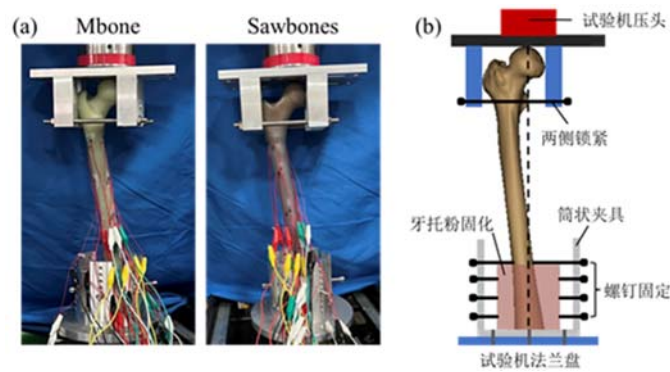


图6 (a) Mbone 股骨与 Sawbones 股骨扭转实验; (b) 扭转固定示意图

Fig. 6 (a) torsion test of Mbone femur and Sawbones femur; (b) torsional fixation diagram

2 结果

2.1 压缩力学性能

(1) 压缩载荷-位移曲线

图7所示为Mbone和Sawbones股骨在压缩载荷下的载荷-位移曲线, Mbone股骨的平均压缩刚度为1585.7N/mm, Sawbones股骨的平均压缩刚度为1479.6N/mm。压缩载荷达到约3500N时, Mbone股骨发生破坏, 出现如图8(a)所示的股骨颈骨折, 骨折形态与图8(b)所示临床中的股骨颈骨折示意图基本一致^[22-23]。

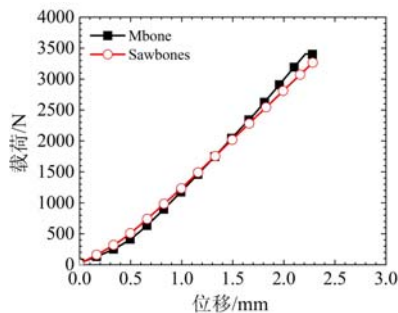


图7 压缩载荷下 Mbone 股骨与 Sawbones 股骨的载荷-位移曲线

Fig. 7 Load-displacement curves of Mbone femur and Sawbones femur under compressive

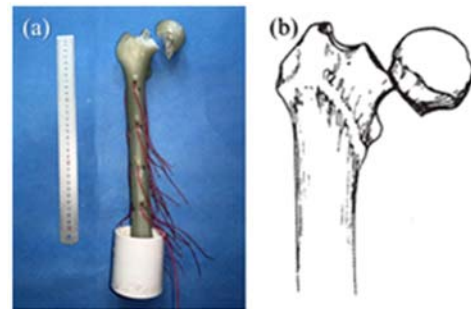


图8 (a) Mbone 股骨压缩破坏; (b) 股骨颈骨折示意图^[22-23]

Fig. 8 (a) Mbone femur compression failure; (b) diagram of femoral neck fracture^[22-23]

(2) 压缩应变分布

图9所示为压缩载荷下Mbone与Sawbones股骨16个分区点位的应变分布, 从图中可以看出2种仿真骨大多数点位的应变值变化趋势与数值基本一致, 只在股骨内侧中段6区有明显不同: 压缩载荷大于500N时, Mbone股骨在该区的应变值逐渐大于Sawbones, 当到达2000N时, Mbone股骨在该区的应变值比Sawbones约高26.3%。

2.2 扭转力学性能

如图10所示, 股骨内旋时, Sawbones股骨的扭转刚度为 $8.9\text{N}\cdot\text{m}/(^{\circ})$, Mbone的平均扭转刚度为 $8.3\text{N}\cdot\text{m}/(^{\circ})$; 股骨外旋时, Sawbones股骨的扭转刚度为 $9.3\text{N}\cdot\text{m}/(^{\circ})$, Mbone的扭转刚度为 $7.6\text{N}\cdot\text{m}/(^{\circ})$ 。

3 讨论

本文通过力学实验研究了Mbone股骨的整骨压缩和扭转力学性能, 并与Sawbones仿真股骨进行

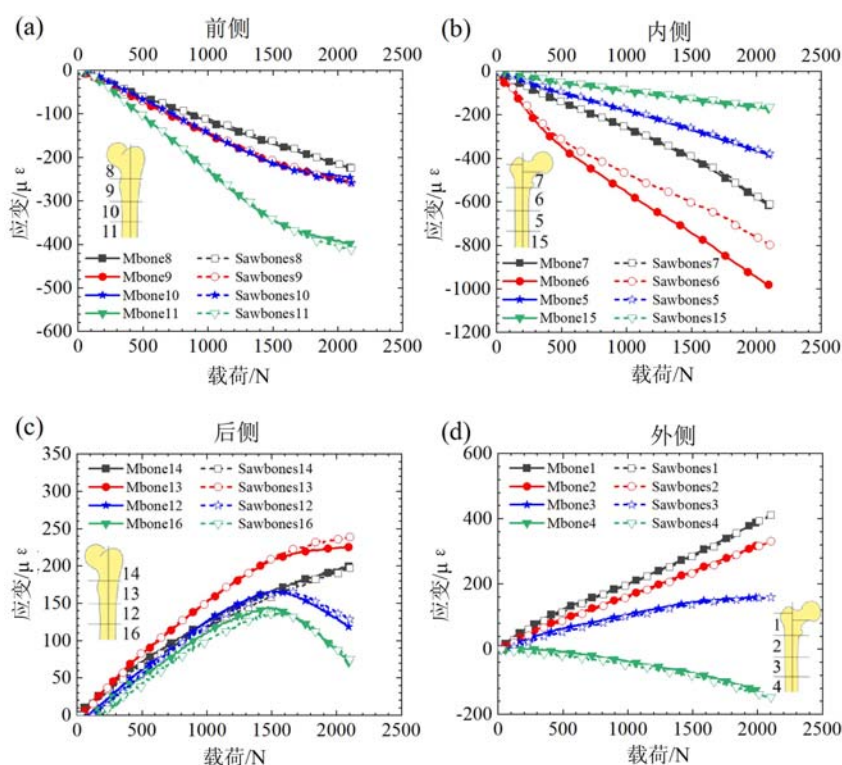
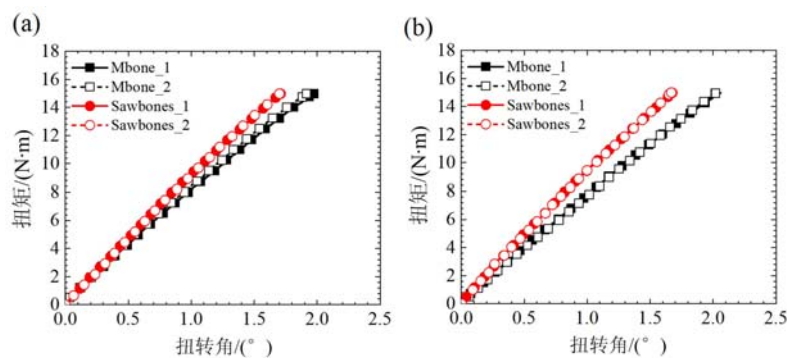


图 9 压缩载荷下 Mbone 与 Sawbones 股骨周围应变分布：

(a)股骨前侧点位；(b)股骨内侧点位；(c)股骨后侧点位；(d)股骨外侧点位

Fig. 9 Strain distribution around Mbones and Sawbones femur under compression:

(a)anterior femur; (b)medial femur; (c)posterior femur; (d)lateral femur



注：Mbone_1、Mbone_2 及 Sawbone_1、Sawbone_2 分别为同一样品的 2 次重复实验。

图 10 扭转载荷下 Mbone 与 Sawbones 股骨的扭矩-转角曲线：(a)内旋工况；(b)外旋工况

Fig. 10 Torque-angle curve of Mbone and Sawbones femur under torsion: (a)internal rotation; (b)external rotation

对比,以验证新型力学等效仿真骨 Mbone 的压缩及扭转力学等效性。

在整骨压缩实验中, Mbone 股骨的平均压缩刚度约比 Sawbones 股骨高 7.2%, 压缩破坏载荷约为 3500N。尸体股骨压缩破坏载荷调研结果见表 1, 以往文献中尸体股骨近端骨折的破坏载荷为 2290N ~ 4710N^[24-25]。尸体骨破坏强度与股骨颈长度、皮质骨厚度、骨质疏松程度等因素相关, 个体差异性较大, 因此调研文献中的破坏载荷范围较大。Mbone 股骨的破坏载荷在文献报道范围内, 而且 Mbone 股骨压缩破坏时出现了与临床中形态基本一致的股骨颈骨折, 因此可认为其压缩破坏强度满足等效性要求。

表1 既往文献尸体股骨压缩破坏载荷调研

Tab.1 Investigation on compression failure load of corpse femur in previous literature

	压缩破坏载荷/N	实验样品	样品数量
TOPP 等 ^[24]	2564~4290	新鲜	6
	2898~4306	防腐	6
GLUEK 等 ^[25]	2290~4710	新鲜	5

压缩实验应变结果显示,除了股骨中段6区,Mbone和Sawbones在压缩过程中的股骨表面应变分布高度一致。6区位于股骨内侧中段偏后方,承受内侧及后侧弯曲压应力和轴向压缩应力。Mbone仿真股骨基于中国人CT数据建立,与Sawbones股骨在前弓角和前倾角上都有明显差异:Mbone股骨前弓角度大,股骨中段弯曲更明显,前侧受拉、后侧和内侧受压程度更高^[26-28];前倾角度大,前侧受拉程度和后侧受压程度减弱。因此可以认为,Mbone股骨6区压应变显著高于Sawbones是由前弓角和前倾角共同作用引起的。

在整骨扭转实验中,内旋时Mbone的平均扭转刚度约比Sawbones股骨低6.7%;外旋时,Mbone股骨的扭转刚度比Sawbones低18.3%。

Mbone股骨的压缩破坏载荷在尸体骨破坏载荷范围内,整体压缩刚度、扭转刚度与Sawbones差距不超过20%,股骨表面多个点位的应变分布均与Sawbones股骨具有较高相似度;由于股骨结构差异,Mbone与Sawbones股骨中段内侧偏后区域的应变值有明显差异。本文研究结果显示,Mbone破坏载荷与尸体骨相当,在整体压缩、扭转刚度及压缩应变分布上能够与Sawbones媲美,且外形结构上比Sawbones更适合中国人骨。

4 结论

为了验证力学等效仿真骨Mbone的压缩及扭转力学等效性,本文研究了Mbone股骨压缩及扭转力学性能,并对比了Mbone股骨与尸体骨、Sawbones股骨的力学性能异同。研究表明:Mbone股骨的压缩破坏载荷在尸体骨合理范围内,整骨压缩刚度、内旋扭转刚度和骨表面压应变分布与Sawbones股骨基本一致,且外形结构比Sawbones更符合中国人骨型。因此,Mbone股骨在压缩及扭转力学性能上均具备良好的力学等效性,可以作为适合中国人的力学等效仿真股骨。

致谢 感谢国家纳米科学中心刘璐琪老师、朱明权同学及王聪颖同学在样品制备方面的帮助。

参考文献:

- [1] ELFAR J, MENORCA R M G, REED J D, et al. Composite bone models in orthopaedic surgery research and education[J]. Journal of the American Academy of Orthopaedic Surgeons, 2014, 22(2):111-120.
- [2] SOMMERS M B, FITZPATRICK D C, MADEY S M, et al. A surrogate long-bone model with osteoporotic material properties for biomechanical testing of fracture implants[J]. Journal of Biomechanics, 2007, 40(15):3297-3304.
- [3] ZDERO R, BRZOZOWSKI P, SCHEMITSCH E H. Biomechanical properties of artificial bones made by Sawbones: a review[J]. Medical Engineering & Physics, 2023, 118:1-15.
- [4] CHONG A C M, MILLER F, BUXTON M, et al. Fracture toughness and fatigue crack propagation rate of short fiber reinforced epoxy composites for analogue cortical bone[J]. Journal of Biomechanical Engineering, 2007, 129(4):487-493.
- [5] GARDNER M P, CHONG A C, POLLOCK A G, et al. Mechanical evaluation of large-size fourth-generation composite femur and tibia models[J]. Annals of Biomedical Engineering, 2010, 38(3):613-620.
- [6] CHONG A C M, FRIIS E A, BALLARD G P, et al. Fatigue performance of composite analogue femur constructs under high activity loading[J]. Annals of Biomedical Engineering, 2007, 35(7):1196-1205.
- [7] LAMB J N, COLTART O, ADEKANMBI I, et al. Comparison of axial-rotational postoperative periprosthetic fracture of the femur in composite osteoporotic femur versus human cadaveric specimens: a validation study[J].

- Proceedings of the Institution of Mechanical Engineers, 2022, 236(7):973–978.
- [8] KEMKER B, MAGONE K, OWEN J, et al. A sliding hip screw augmented with 2 screws is biomechanically similar to an inverted triad of cannulated screws in repair of a pauwels type-III fracture[J]. Injury-International Journal of the Care of the Injured, 2017, 48(8):1743–1748.
- [9] KARAKASLI A, BASCI O, ERTEM F, et al. Dual plating for fixation of humeral shaft fractures; a mechanical comparison of various combinations of plate lengths[J]. Acta Orthopaedica et Traumatologica Turcica, 2016, 50(4):432–436.
- [10] WEGMANN K, ENGEL K, SKOURAS E, et al. Reconstruction of monteggia-like proximal ulna fractures using different fixation devices: a biomechanical study[J]. Injury-International Journal of the Care of the Injured, 2016, 47(8):1636–1641.
- [11] CROOK P D, OWEN J R, HESS S R, et al. Initial stability of cemented vs cementless tibial components under cyclic load[J]. Journal of Arthroplasty, 2017, 32(8):2556–2562.
- [12] BREDOW J, MEYER C, SCHEYERER M J, et al. Accuracy of 3D fluoroscopy-navigated anterior transpedicular screw insertion in the cervical spine; an experimental study[J]. European Spine Journal, 2016, 25(6):1683–1689.
- [13] 姜滔, 吕一, 沈建国, 等. Sawbones 人工合成骨和尸体骨的生物力学比较研究[J]. 中医正骨, 2010, 22(5):15–18 (JIANG Tao, LÜ Yi, SHEN Jianguo, et al. A biomechanical comparison between composite bones and cadaver femoral bone[J]. The Journal of Traditional Chinese Orthopedics and Traumatology, 2010, 22(5):15–18 (in Chinese))
- [14] 金乾坤, 王巍, 何盛为, 等. 股骨有限元模型材料属性分配梯度的优化分析[J]. 中国生物医学工程学报, 2020, 39(1):84–90 (JIN Qiankun, WANG Wei, HE Shengwei, et al. The optimized analysis on the distribution gradient of material attributes of femur finite element model[J]. Chinese Journal of Biomedical Engineering, 2020, 39(1):84–90 (in Chinese))
- [15] TSUBOTA K, ADACHI T, TOMITA Y. Functional adaptation of cancellous bone in human proximal femur predicted by trabecular surface remodeling simulation toward uniform stress state[J]. Journal of Biomechanics, 2002, 35(12):1541–1551.
- [16] CHEN H, KUBO K-Y. Bone three-dimensional microstructural features of the common osteoporotic fracture sites [J]. World Journal of Orthopedics, 2014, 5(4):486–495.
- [17] 张海峰, 宋翠荣, 刘媛媛, 等. 股骨标本形态参数的三维重建测量与直接测量比较分析[J]. 中国临床医学影像杂志, 2017, 28(11):825–828 (ZHANG Haifeng, SONG Cuirong, LIU Yuanyuan, et al. Comparative analysis of 3D reconstruction measurement of morphological parameters of femoral specimens with direct measurement[J]. Journal of China Clinic Medical Imaging, 2017, 28(11):825–828 (in Chinese))
- [18] 左建林, 柳林, 应洪亮, 等. 基于三维 CT 多平面重建股骨近段髓腔的形态学实验[J]. 中国组织工程研究与临床康复, 2010, 14(22):4005–4009 (ZUO Jianlin, LIU Lin, YING Hongliang, et al. Multiple-plane reconstruction of the proximal femoral canal using three-dimensional CT scans: a morphological study[J]. Chinese Journal of Tissue Engineering Research, 2010, 14(22):4005–4009 (in Chinese))
- [19] MAHAISAVARIYA B, SITTHISERIPRATIP K, TONGDEE T, et al. Morphological study of the proximal femur: a new method of geometrical assessment using 3-dimensional reverse engineering[J]. Medical Engineering & Physics, 2002, 24(9):617–622.
- [20] COQUIM J, CLEMENZI J, SALAHI M, et al. Biomechanical analysis using FEA and experiments of metal plate and bone strut repair of a femur midshaft segmental defect[J]. Biomed Research International, 2018, 2018:1–11.
- [21] HEINER A D, BROWN T D. Structural properties of a new design of composite replicate femurs and tibias[J]. Journal of Biomechanics, 2001, 34(6):773–781.
- [22] GARDEN R S. Low-angle fixation in fractures of the femoral neck[J]. Journal of Bone and Joint Surgery-british Volume, 1961, 43:647–663.
- [23] 顾立强. 股骨近端骨折的分类与功能评价[J]. 中华创伤骨科杂志, 2004(5):83–88 (GU Liqiang. Classification and functional assessment of the proximal femoral fractures[J]. Chinese Journal of Orthopaedic Trauma, 2004(5): 83–88 (in Chinese))

- [24] TOPP T, MÜLLER T, HUSS S, et al. Embalmed and fresh frozen human bones in orthopedic cadaveric studies: which bone is authentic and feasible? [J]. *Acta Orthopaedica*, 2012, 83(5):543–547.
- [25] GLUEK C, ZDERO R, QUENNEVILLE C E. Evaluating the mechanical response of novel synthetic femurs for representing osteoporotic bone[J]. *Journal of Biomechanics*, 2020, 111:1–6.
- [26] HAIDER I T, SCHNEIDER P, MICHALSKI A, et al. Influence of geometry on proximal femoral shaft strains: implications for atypical femoral fracture[J]. *Bone*, 2018, 110:295–303.
- [27] OH Y, FUJITA K, WAKABAYASHI Y, et al. Location of atypical femoral fracture can be determined by tensile stress distribution influenced by femoral bowing and neck-shaft angle: a CT-based nonlinear finite element analysis model for the assessment of femoral shaft loading stress[J]. *Injury-International Journal of the Care of the Injured*, 2017, 48(12):2736–2743.
- [28] TANO A, OH Y, FUKUSHIMA K, et al. Potential bone fragility of mid-shaft atypical femoral fracture: biomechanical analysis by a CT-based nonlinear finite element method[J]. *Injury-International Journal of the Care of the Injured*, 2019, 50(11):1876–1882.

Compression and torsion biomechanical equivalence study of Mbone

LI Yu^{1,2}, XIN Peng³, LIU Moyu^{2,4}, WANG Zhixuan², WANG Jun^{2,4,5}, HUAN Yong^{2,4}

(1. College of Engineering, China Agricultural University, Beijing 100083, China; 2. State Key Laboratory of Nonlinear Mechanics, Institute of Mechanics, Chinese Academy of Sciences, Beijing 100190, China; 3. Department of Orthopaedics, General Hospital of Southern Theater Command of PLA, Guangzhou 510010, Guangdong, China; 4. School of Engineering Science, University of Chinese Academy of Sciences, Beijing 100049, China; 5. Research Center for Frontier Fundamental Studies, Zhejiang Lab, Hangzhou 311121, Zhejiang, China)

Abstract: Cadaver bone is often used in clinic and bone biomechanical research, but its samples are scarce and the consistency between samples is poor. Therefore, a simulated bone with mechanical equivalence to cadaver bone is indispensable. Sawbones is currently the most recognized artificial bone with mechanical equivalence, but it is developed based on the American bones, which is quite different from the Chinese bones, especially the femoral anteversion and anterior arch of the femur. The purpose of this paper is to research the compressive and torsional mechanical properties of the new Chinese mechanical equivalent simulation bone Mbone femur by biomechanical test, and to verify its mechanical equivalence. In this paper, the compression and torsion mechanical properties of the Mbone femur and Sawbones femur were tested and compared. Results showed that the compressive stiffness of Mbone femur was slightly 7.2% higher than that of Sawbones, and its compressive failure load was within the range of cadaver bones. After destruction, it presented a femoral neck fracture that was consistent with clinical cases. The posterior compressive strain in the middle of the medial femur of Mbone was significantly higher than that of Sawbones, and the compressive strain in the other 15 regions was highly consistent with that of Sawbones. When subjected to torsion, the inward torsional stiffness of Mbone femur was slightly 6.7% lower than that of Sawbones and the outward torsional stiffness was significantly lower than that of Sawbones. Mbone femur showed satisfactory mechanical equivalence in compression and torsion mechanical properties, and was more suitable for Chinese bone. Therefore, it is considered that it can replace imported products as mechanical equivalent samples of cadaver bone.

Keywords: mechanical equivalence; compression; torsion; Mbone; Sawbones; femur